Multi-Modal Deep Learning Framework Integrating DSP-Processed Mammograms and Clinical–Histopathological Features for Benign Breast Tumor Subclassification

Shahinur Rahman [1*]

1 Department of Electrical and Electronic Engineering , Faculty of Science and Technology, City University, Bangladesh, Khagan, Savar, Dhaka, Bangladesh

* Corresponding author,e-mail: shahinurislamkowser@gmail.com

Abstract

In this paper, we propose a new multimodal deep learning framework for subclassification of benign breast tumors, which fuses clinical, histopathological, and mammogram image information. The method incorporates a lot of digital signal processing (DSP) solutions in the field of image preprocessing and feature extraction. First-level processing contains noise removal (median filter, Gaussian filter), contrast enhancement (CLAHE, histogram equalization), standardization of intensity, and rescaling. Advanced DSP techniques such as FFT, DWT, and GLCM/LBP are used to extract frequency-domain, time-frequency texture, and local or global characteristics of mammograms. Imputation and one-hot encoding of clinical data. All the characteristics are finally concatenated, and dimensionality is reduced using Principal Component Analysis (PCA), leaving 16 components that express 95% of the variance. Furthermore, a DSP-domain augmentation (frequency noise, wavelet perturbation) increases the amount of data in the dataset. We trained an MLP model on these reduced features, resulting in a test accuracy of 1.0000 and a loss of 0.0116. It is proven that this framework performs effectively in benign breast tumor subclassification, indicating a significant strength of integrated multi-modal data and advanced DSP for the medical image analysis, though more validations on larger databases are encouraged.

Keywords:

Benign Breast Tumor Subclassification; Breast Tumor; Digital Signal Processing (DSP); Mammogram Image Analysis; Medical Image Processing.

1 INTRODUCTION

Breast cancer continues to be one of the leading causes of death in women all over the world; thus, for proper treatment and prognosis, accurate early diagnosis and subclassification of breast lesions are critically important. Although there is much focus on malignant tumors, benign breast tumors create a variety of diagnostic problems as well. Lesions that are benign but often simulate malignancy radiologically and/or clinically may cause unnecessary biopsies or emotional stress in the patient. In addition, some of these benign proliferative entities have higher associated risks or subsequent risks of transformation to malignancy and therefore also require careful subclassification for targeted management and surveillance algorithms.

Common procedures to subclassify benign breast tumors are based on invasive histopathological scrutinizing and subjective radiological image interpretation. The multi-modal data fusion between complementary information sources (clinical history, histopathological features, and advanced imaging characteristics on mammograms) could be of great value for improving the diagnosis and understanding of these lesions. Yet, deriving useful information from the combination of these heterogeneous applications is extremely technically demanding.

In this paper, we present a new multimodal deep learning framework with the purpose of accurately subclassifying benign breast tumors. To the best of our knowledge, our methodology exploits deep digitally sound signal processing (DSP) frameworks to extract relevant and quantitative features from digital images referred to as mammograms, including frequency-domain, time-frequency, texture, morphology, and region of interest (ROI). The image-based DSP features are subsequently combined with clinic and pathology data. In order to tackle the problem of small dataset size in medical imaging, we also propose DSP-domain data augmentation techniques. The resulting combined and dimensionality-reduced feature set is then processed in a deep learning way by passing through a multilayer perceptron (MLP) for classification. In this study, we developed a framework to illustrate how integration of the two cutting-edge technologies—advanced DSP and DL—can lead to better accuracy of subclassification as well as robustness for benign breast tumor classification, benefiting clinical decision-making.

2 Dataset Description

In the present study, data from 83 Indian patients along with their clinical, histopathological, and mammographic findings are used [1]. The unique attribute of the dataset is that it concentrates on benign tumors, and the mammograms were acquired for subclassifying benign lesions. This dataset consists of a ZIP package that contains 80 mammographic images and an Excel file with mammographic findings, histological diagnoses, and clinical information (age and menopause) that is available for all patients. This multi-instrument dataset enables extensive study of benign breast tumor subtypes through incorporation of imaging with clinical and pathology characteristics.

3 Overall Multi-Modal Deep Learning Framework Architecture

This architecture, shown in Fig. 1, offers a multi-modality deep learning pipeline for benign breast tumor subtype classification by including clinical, histopathological, and mammographic images. There are several main stages to the process:

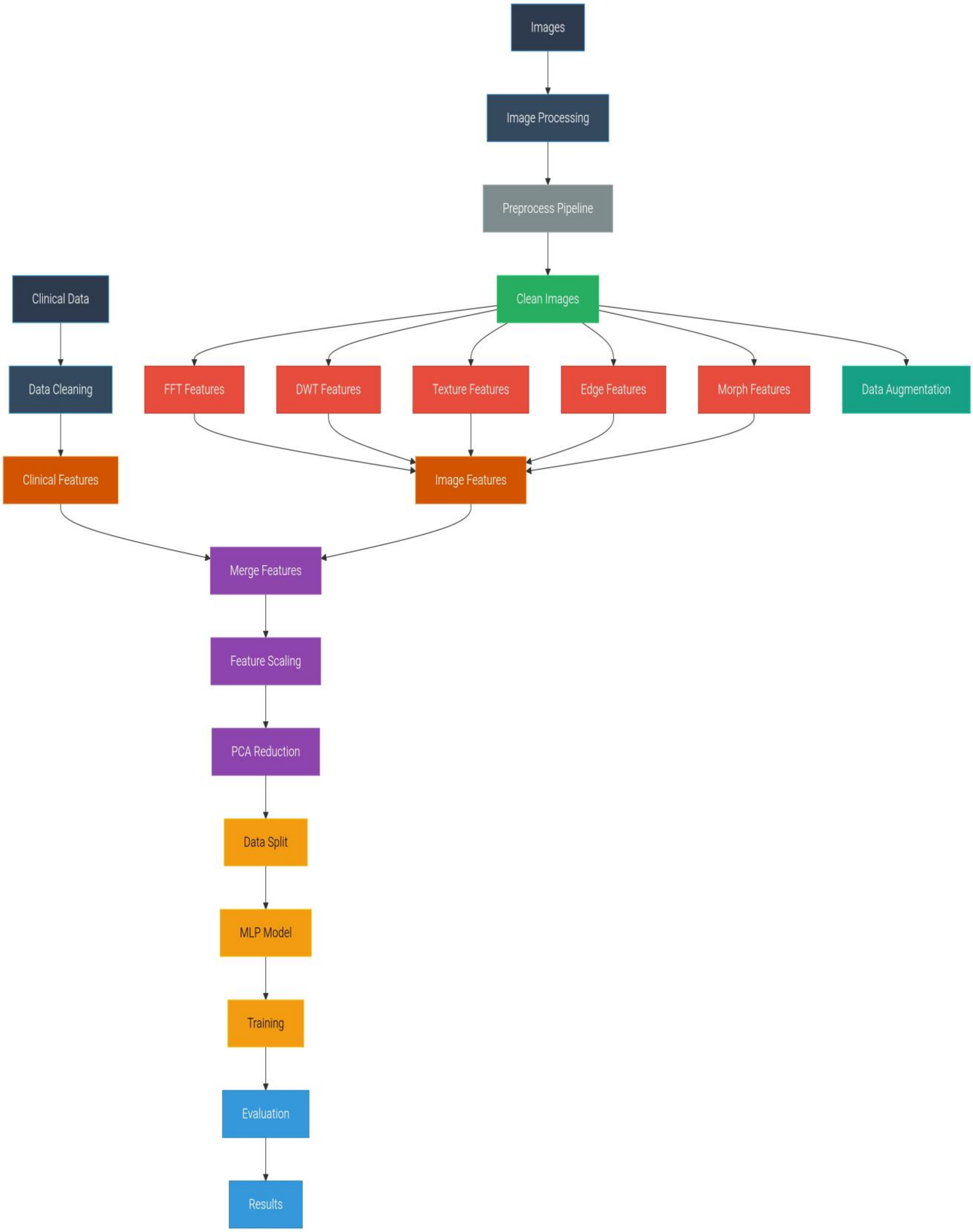

Fig. 1 Overall Multi-Modal Deep Learning Framework Architecture

- Data Acquisition and Initial Preprocessing: We obtained clinical data from 'Clinical_Attributes.xlsx.' The dataset is preprocessed by handling missing data (numerical columns—replaced with median) and converting categorical columns to one-hot encoding. Mammogram images from 'Dataset.zip' are extracted and organized.

- Image Pre-processing (DSP Domain): Raw mammograms are processed by digital signal processing in detail for enhancement. This can be seen in converted grayscale; instead of mean and Gaussian filtering (5 x 5 kernels), contrast and noise reduction were obtained by CLAHE and histogram equalization, respectively, and intensity normalization (0 to 255) as well as resizing to (256 x 256) pixels. These preprocessed images are saved.

- Advanced Feature-Oriented DSP: A comprehensive set of quantitative features is computed from preprocessed mammograms. This comprises Frequency-Domain (2D FFT mean/std), Time-Frequency (DWT 'haar' wavelet coeff. mean/std), Texture (GLCM properties, LBP mean/std), Spatial-Domain (Canny edge pixels, LoG mean absolute response), and Morphological/ROI features (Area, Perimeter, Compactness, Eccentricity, and Major/Minor Axis Length from Otsu-thresholded, connected-component identified ROIs).

- Feature Integration and Reduction: The entire DSP-derived image features are concatenated with the standardized clinical and histopathological features for all patients over 'P_Code.' The fused feature set is processed by PCA to reduce dimensions into 16 principal components that explain around 95% of the total variability.

- DSP-Domain Data Augmentation: Data Augmentation Due to the scarcity of data, we directly perform DSP-domain data augmentation on the preprocessed image. Augmentation techniques: injecting Gaussian noise into the higher-pass elements in the Fourier transform and adding noisy coefficients of detail in DWT (they produce 160 synthetic images from the 80 original ones).

- Multi-Modal Deep Learning Model: A model of Multi-Layer Perceptron (MLP) is created. It takes as input the 16 PCA-reduced features, then two hidden 'Dense' layers (128 and 64 neurons, ReLU activation, 0.3 Dropout after each). The output layer is an 8-neuron Softmax activation for multi-class classification. The model is trained using the Adam optimizer, categorical cross-entropy loss, and accuracy metric. Training is performed with 100 epochs, a batch size of 8, and using EarlyStopping and ModelCheckpoint callbacks.

- Performance Evaluation: The trained model reaches a test loss of 0.0116 and a test accuracy of 1.0000 on the hold-out test set.

4 Image Preprocessing

Pre-processing mammogram images through early digital signal processing techniques for noise removal and image enhancement. This could be median filtering, Gaussian filtering, adaptive filtering, CLAHE (Contrast Limited Adaptive Histogram Equalization), histogram equalization, intensity normalization, and resizing of the image.

4.1 Original grayscale image

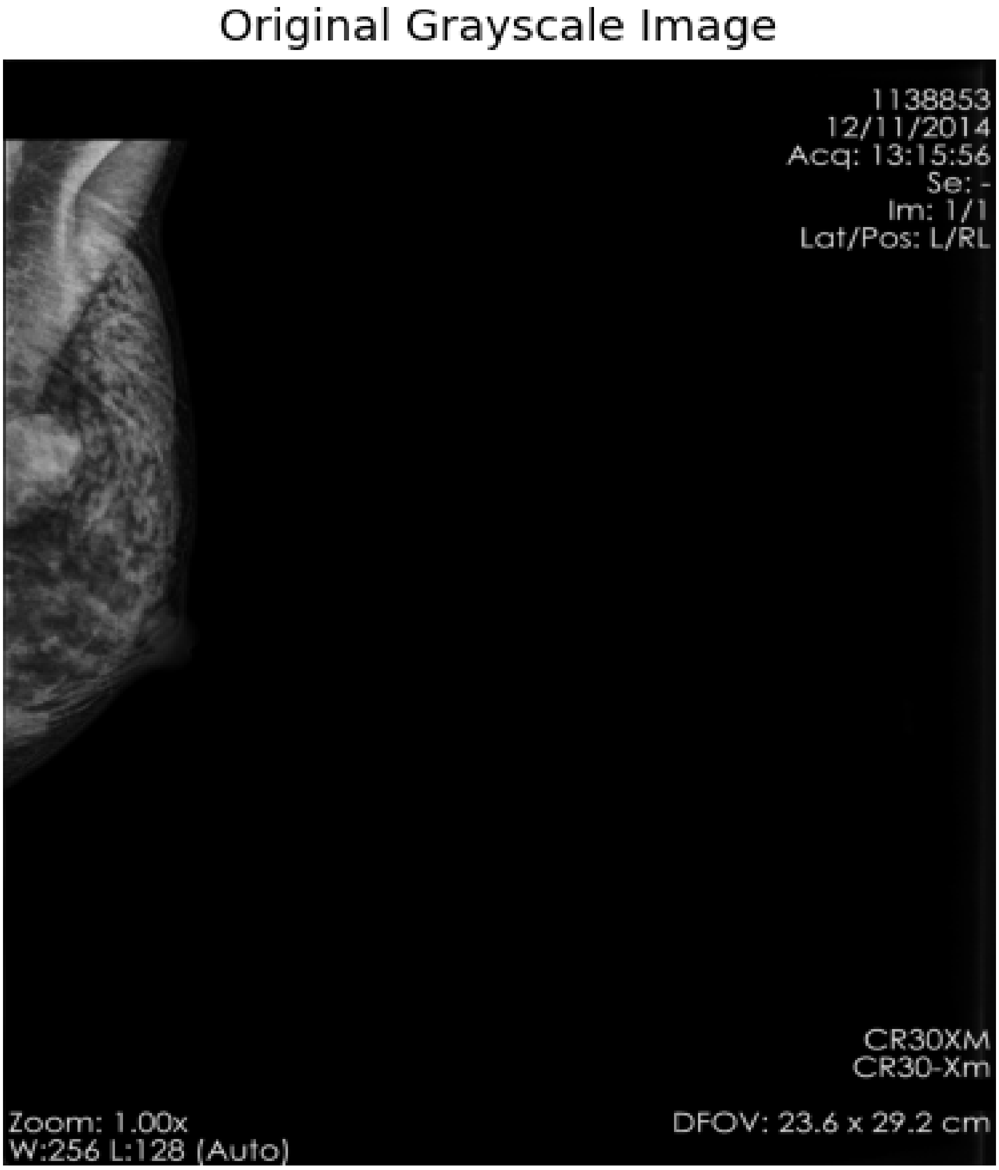

Fig. 2 Original grayscale image [1]

The raw mammographic images were loaded and assembled into grayscale, shown in Fig. 2, immediately before any operations of DSP. This first processing step was able to equalize the image format and to decrease computational effort by considering intensity information only and provided a basic visual model for further preprocessing and feature extraction steps in our multi-modal deep learning architecture.

4.2 Noise reduction techniques (median and Gaussian filtering)

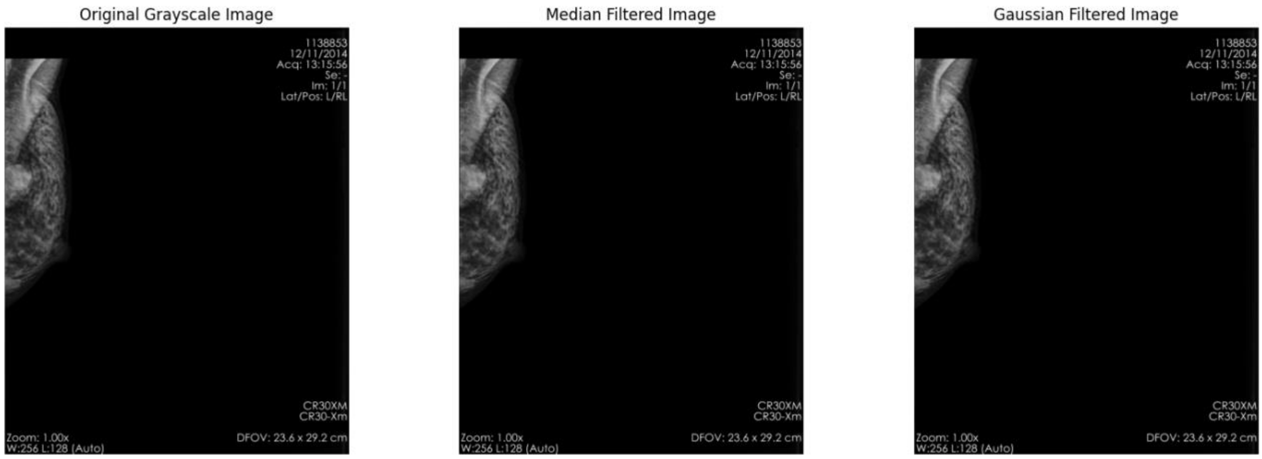

Fig. 3 Noise reduction techniques (median and Gaussian filtering)

Before high-level feature extraction, the mammogram images were first substantially noise reduced to ensure the quality of the signal and removal of artifacts, which is critical for rigorous analysis. Two main strategies we used are median filtering and Gaussian filtering, which are shown in Fig. 3. Median filtering is a nonlinear digital filtering method that excels at removing salt-and-pepper and similar impulsive noise while preserving edges. It works by replacing each pixel's value with the median of the values of its neighboring pixels, including itself, inside a defined kernel (3 x 3, 5 x 5, etc.). Unlike averaging, this approach suppresses the influence of substantial outlier pixel values on the output and results in smoother results without losing sharp features in anatomical structures as radically. However, Gaussian filtering is a straightforward smoothing filter to essentially blur the details of the image and reduce noise by applying a convolution between an image and a Gaussian function. The kernel is weighted according to a Gaussian distribution with higher weight applied to the pixels near to the center of the kernel (e.g., for a 5x5 kernel and std dev=1). The method is very effective for noise removal by adapting its smoothing effect, preferable whenever it is necessary to prepare images for contrast enhancement or segmentation steps by attenuating high-frequency irregularities. They both contribute to the computational efficiency and visual quality of the mammogram data.

4.3 Contrast enhancement techniques (CLAHE and histogram equalization)

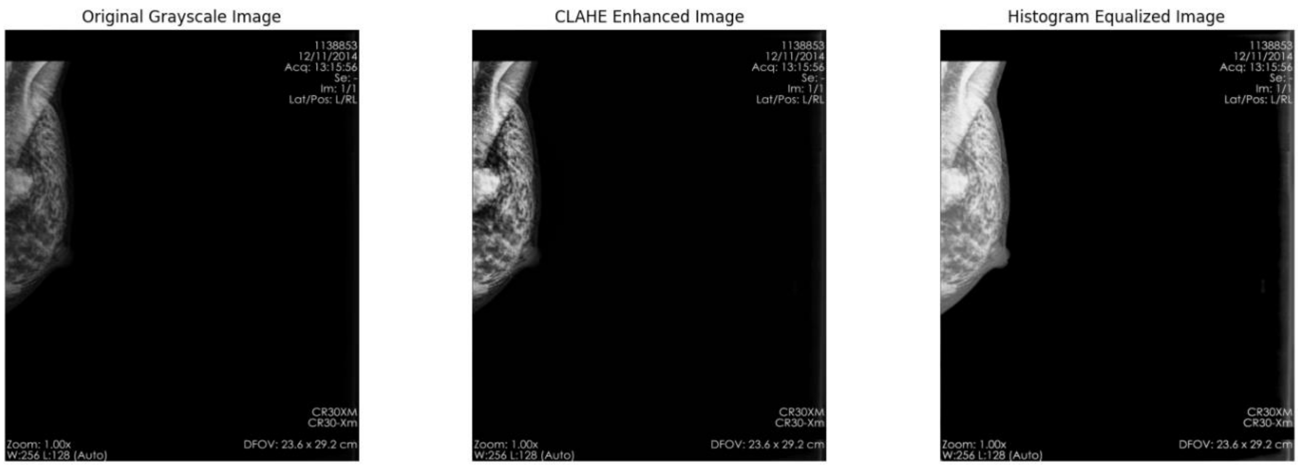

Fig. 4 Contrast enhancement techniques (CLAHE and histogram equalization)

In image pre-processing, Histogram Equalization (HE), shown in Fig. 4, is a global contrast enhancement technique that attempts to redistribute the most frequent pixel intensity values and expand the dynamic range so that it covers a given target interval. However, the Histogram Equalization (HE) has the deficiency of over-enhanced noise and unnatural images due to its global method. To solve this, Contrast Limited Adaptive Histogram Equalization (CLAHE) has been used, which is shown in Fig. 4. Contrast Limited Adaptive Histogram Equalization (CLAHE) works on small regions of an image, not the whole image, and is sensitive to variations in local contrast. This type of adaptive processing should avoid over-processing the homogenous regions. A noteworthy attribute of CLAHE is that it has a clipLimit parameter, which limits the contrast enhancement to avoid noise amplification in individual local ROIs, which is normally set as 2.0. Moreover, the image is split into a tileGridSize, for example (8, 8), to process these local regions independently, and then the neighboring tiles are merged with bilinear interpolation to remove artificially introduced borders.

4.4 Intensity normalization and resizing

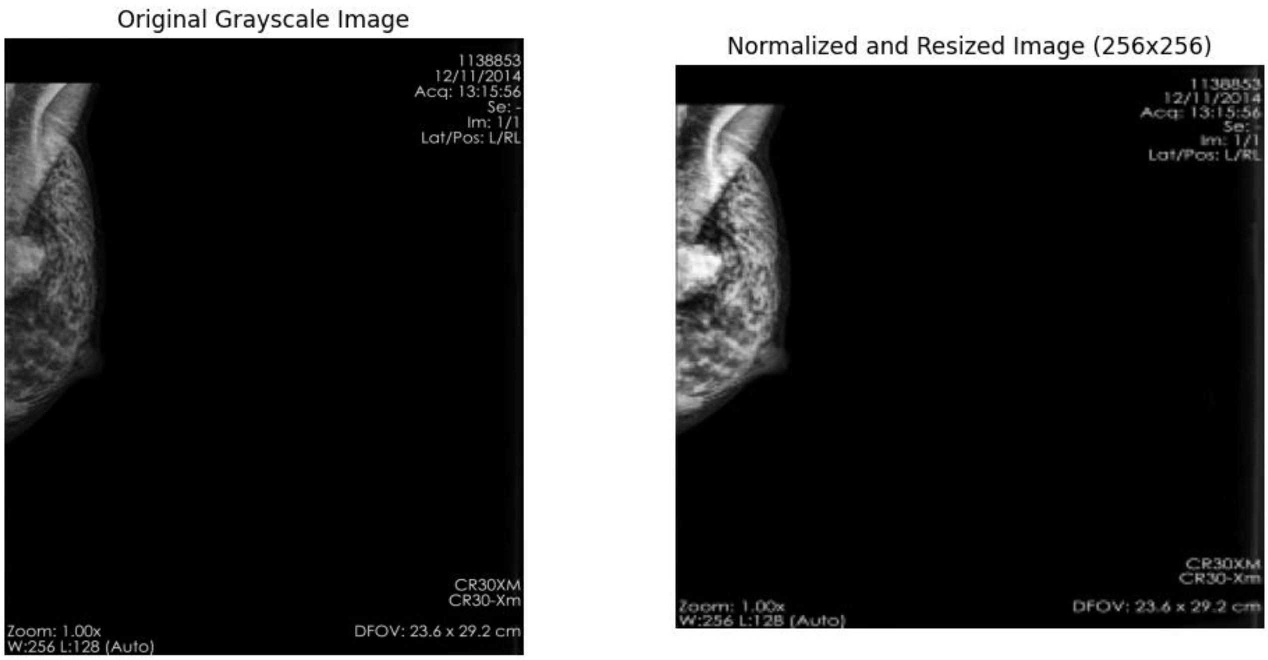

Fig. 5 Intensity normalization and resizing

Intensity normalization, shown in Fig. 5, is an important preprocessing step that linearly scales the pixel values of each image to a specified common range, generally from 0 to 255 in the case of 8-bit images or from 0 (minimum intensity) to 1 (maximum intensity) in the case of float representation. Such a process aids in alleviating differences in illumination, sensibility, or parameter acquisition between images to avoid the model overemphasizing features according to arbitrary intensity scales. Normalization helps feature extraction remain consistent, and it helps with the robustness and speed of convergence in deep learning models. At the same time, image resizing resizes images into a homogeneous spatial dimension, e.g., (256 x 256) pixels, which is necessary to generate fixed-size input tensors, as most CNN architectures demand. Techniques like cv2.INTER_AREA interpolation are often suggested for downsampling because they will handle averaging the pixels in a local area, which makes the image more stable and leads to fewer artifacts due to aliasing. This constant size allows for batched presentation and efficient memory usage for model training and inference.

5 Advanced Digital Signal Processing Techniques

Advanced DSP techniques are then used to extract informative features in the preprocessed mammograms. This includes Frequency-Domain DSP Techniques (e.g., Fast Fourier Transform (FFT), Power Spectral Density (PSD)), Time–Frequency DSP Techniques (e.g., Discrete Wavelet Transform (DWT)), Texture Feature Extraction (e.g., Gray Level Co-Occurrence Matrix, Local Binary Pattern), and Spatial-Domain Filtering & Edge Detection (e.g., Canny Edge Detection, Laplacian of Gaussian).

5.1 Frequency-Domain DSP (FFT and Magnitude Spectrum)

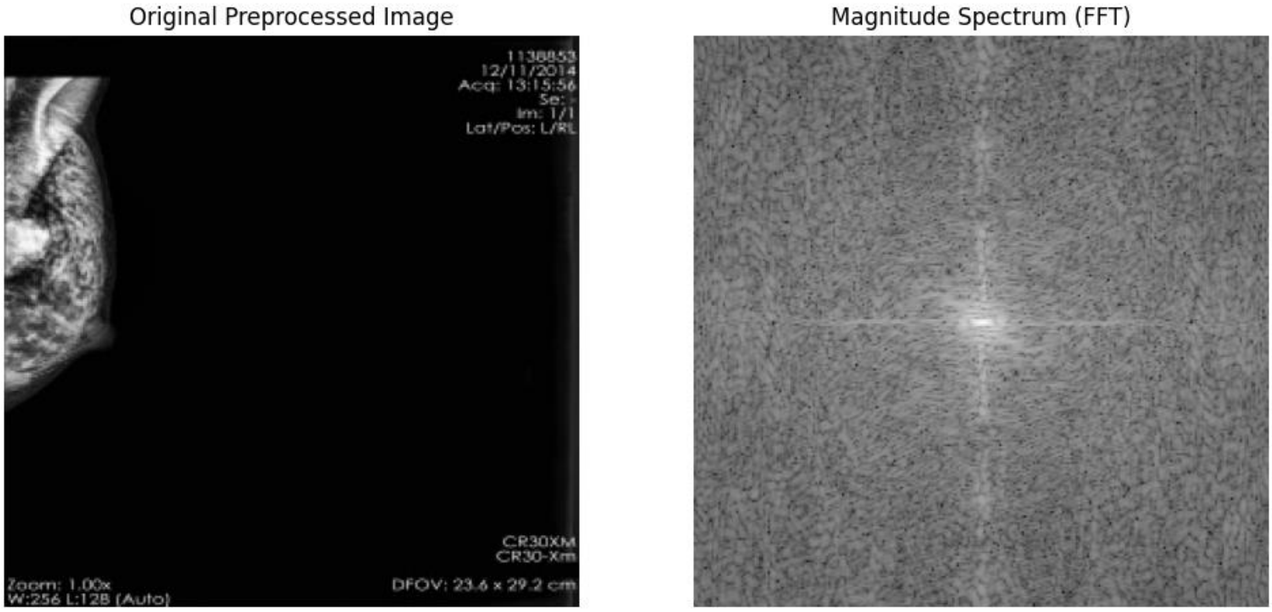

Fig. 6 Frequency-Domain DSP (FFT and Magnitude Spectrum)

Fast Fourier Transform (FFT) was used to transform the spatial image to its frequency domain, which is shown in Fig. 6. This transform shows the dominating frequency components in the mammogram. This magnitude spectrum, shown in Fig. 6, is computed directly from the FFT and represents energy distributed over frequencies. Low-frequency information, such as coarse structures and overall image intensity, is located in the center of these images, while high-frequency information, including fine details, textures, and edges, is found towards the border. The understanding of this spectrum may lead to the joint features, such as texture, homogeneity, or structural patterns, shown in tumor subtyping.

5.2 Time-Frequency DSP (Discrete Wavelet Transform - DWT)

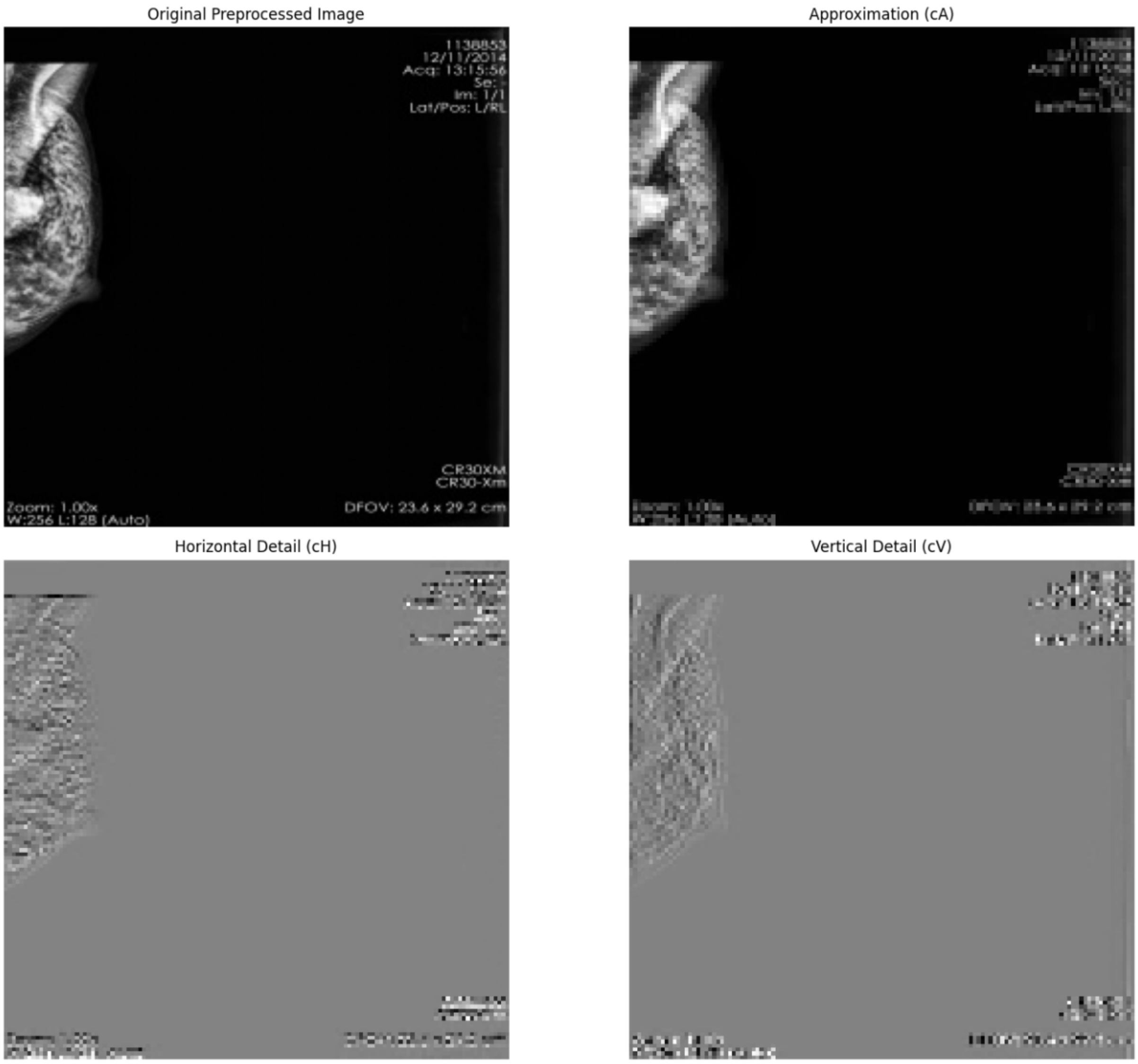

Fig. 7 Time-Frequency DSP (Discrete Wavelet Transform - DWT)

Both time (spatial) and frequency domain Discrete Wavelet Transform (DWT) were used to analyze the image, which are shown in Fig. 7. DWT is a multi-resolution representation that decimates the image into different frequency sub-bands, such as the 'Haar' wavelet. The approximation coefficients (cA) shown in Fig. 7, represent low-frequency information, i.e., the general structure and mean intensity of the image, while the detail coefficients (cH and cV) shown in Fig. 7, represent high-frequency details corresponding to horizontal edge patterns and vertical edge patterns, respectively. This offline scheme is found to be capable of detecting focal features on different scales, an important feature for recording fine patterns of a tumor.

5.3 GLCM Texture Feature Extraction

GLCM analysis was implemented for computation of rotation-invariant second-order texture features that define the statistical relationships between pixel intensities. GLCMs at various distances and angles are calculated to record the commonness with which two gray-level pixels co-occur in an image. From these matrices, a set of discriminative texture descriptors were obtained, including contrast (local intensity variation), dissimilarity (difference between gray levels within neighboring pixels), homogeneity (closeness of the GLCM elements to the diagonal), energy (textural uniformity),

correlation (linear dependency of gray levels among neighboring pixels), and angular second moment (ASM) overall image homogeneity. This texture pattern in breast tissue plays a key role for its characterization and to capture the subtle structural variations corresponding to benign breast tumor patterns.
The values of the extracted GLCM texture feature for a typical sample are shown here: Contrast = 352.6821, Dissimilarity = 5.0261, Homogeneity = 0.8076, Energy = 0.7601, Correlation = 0.8791, and ASM = 0.5778.

5.4 Texture Feature Extraction (LBP)

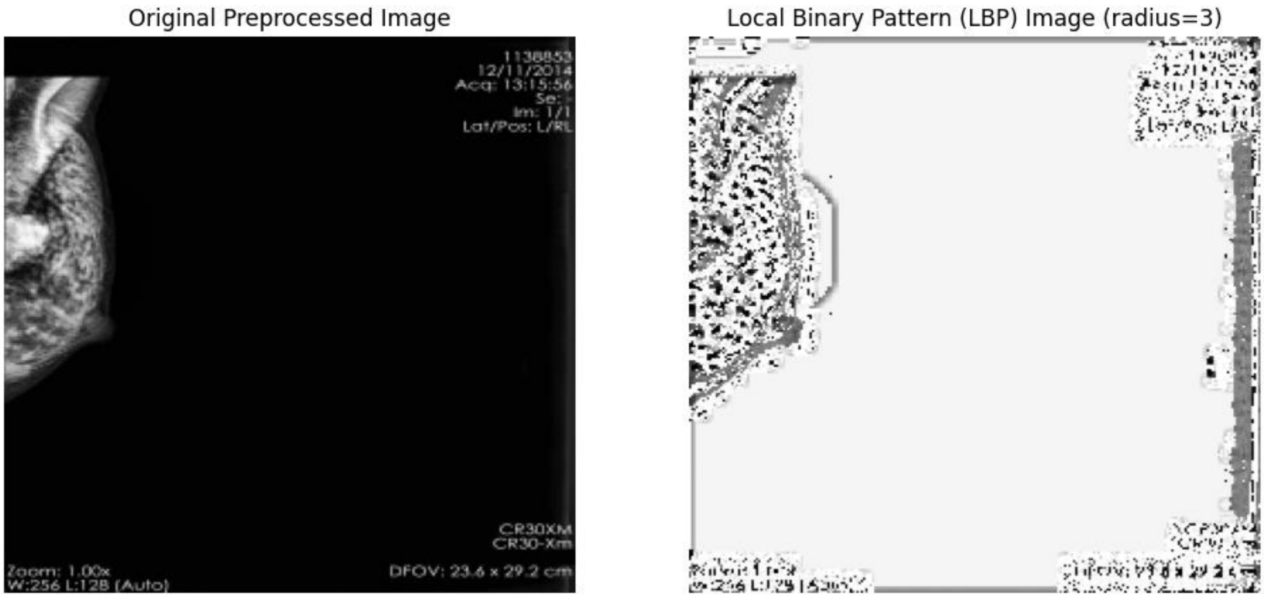

Fig. 8 Texture Feature Extraction (LBP)

The LBP shown in Fig. 8, captured the local image texture such that each pixel value is thresholded with its neighborhood in order to be represented as a binary number. In particular, for all pixels we used n_points = 8 * radius neighbors were considered at a radius = 3. The 'uniform' method was used to evaluate the LBP image, which emphasizes the patterns with at most two bitwise transitions from 0 to 1 or vice versa, and it is rotation-invariant and reduces the number of patterns. The average and standard deviation of the generated LBP image were computed as numerical features. These LBP features efficiently represent local micro-patterns (e.g., edges, lines, and spots), which are the basic descriptors for capturing textural patterns in mammogram images.

5.5 Spatial-Domain Filtering & Edge Detection (Canny, LoG)

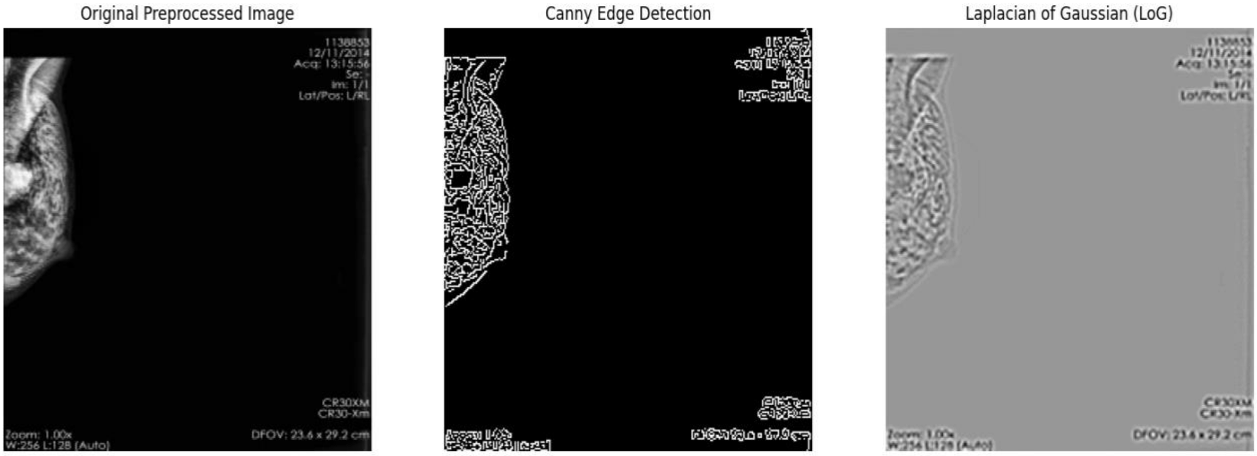

Fig. 9 Spatial-Domain Filtering & Edge Detection (Canny, LoG)

Canny Edge Detection, shown in Fig. 9, was first conducted to detect large intensity gradient changes, which define the borders of objects and are located on the preprocessed mammographic image. It's a multi-stage algorithm used in computer vision processes such as smoothing (Gaussian), calculating gradient, non-maximum suppression theorem, and hysteresis thresholding with the following arguments: low_threshold = 100, high_threshold = 200 to get good edge detection. The sum of edge pixels detected was used as a feature, representing the structural complexity of the image. Meanwhile, the Laplacian of Gaussian (LoG) filter, shown in Fig. 9, was used for edge enhancement and blob detection. This filter first blurs the image with a 5x5 Gaussian kernel and then computes the Laplacian of it to locate rapid intensity change. The average absolute value of the LoG response was used as a feature, offering information on the general edge and detail richness, which can be reflective of tumor structure and texture.

5.6 Morphological Operations

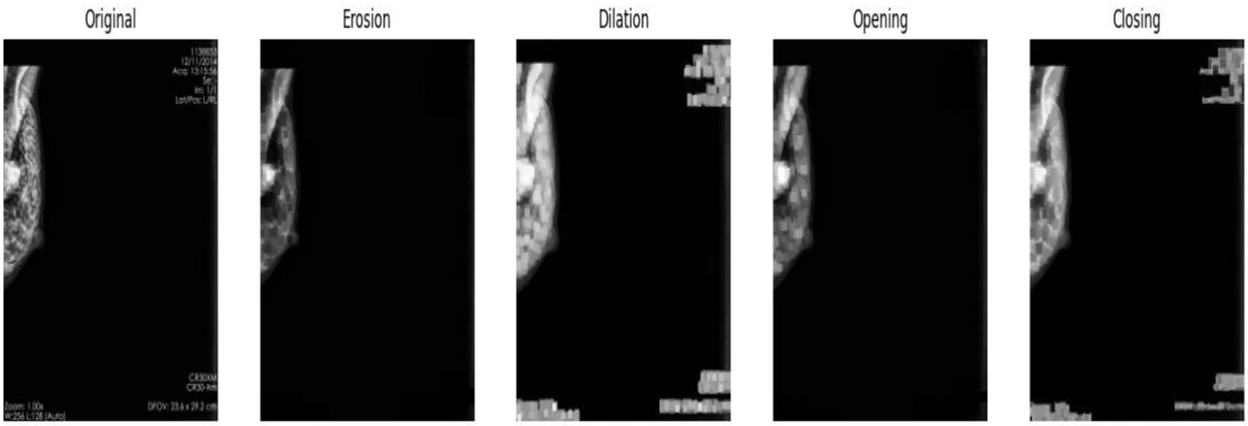

Fig.10 Morphological Operations

The Otsu's method was used to find an optimal global threshold value of 68.0 for binarizing the images. Then, the morphological operations, shown in Fig. 10, was used to change the shape of objects and to emphasize structural information as well with a 5×5 kernel. Erosion, shown in Fig. 10, was used to decrease the size of foreground regions by eliminating small spurious noise and breaking up weakly linked objects. By contrast, dilation, shown in Fig. 10, dilated the boundaries of objects and hence filled in little holes between regions of contiguous pixels while also closing narrow gaps that may exist between those regions. Fig. 10 shows, opening (erosion followed by dilation) was applied to remove small, isolated objects and smooth boundaries of the objects, while closing (dilation followed by erosion), shown in Fig.

10, filled in internal holes or narrow gaps within objects. These operations are critical for improving the quality of the segmented regions before feature extraction in order to have good quantification and discrimination of possible tumor shapes and sizes.

5.7 ROI Identification and Property Extraction

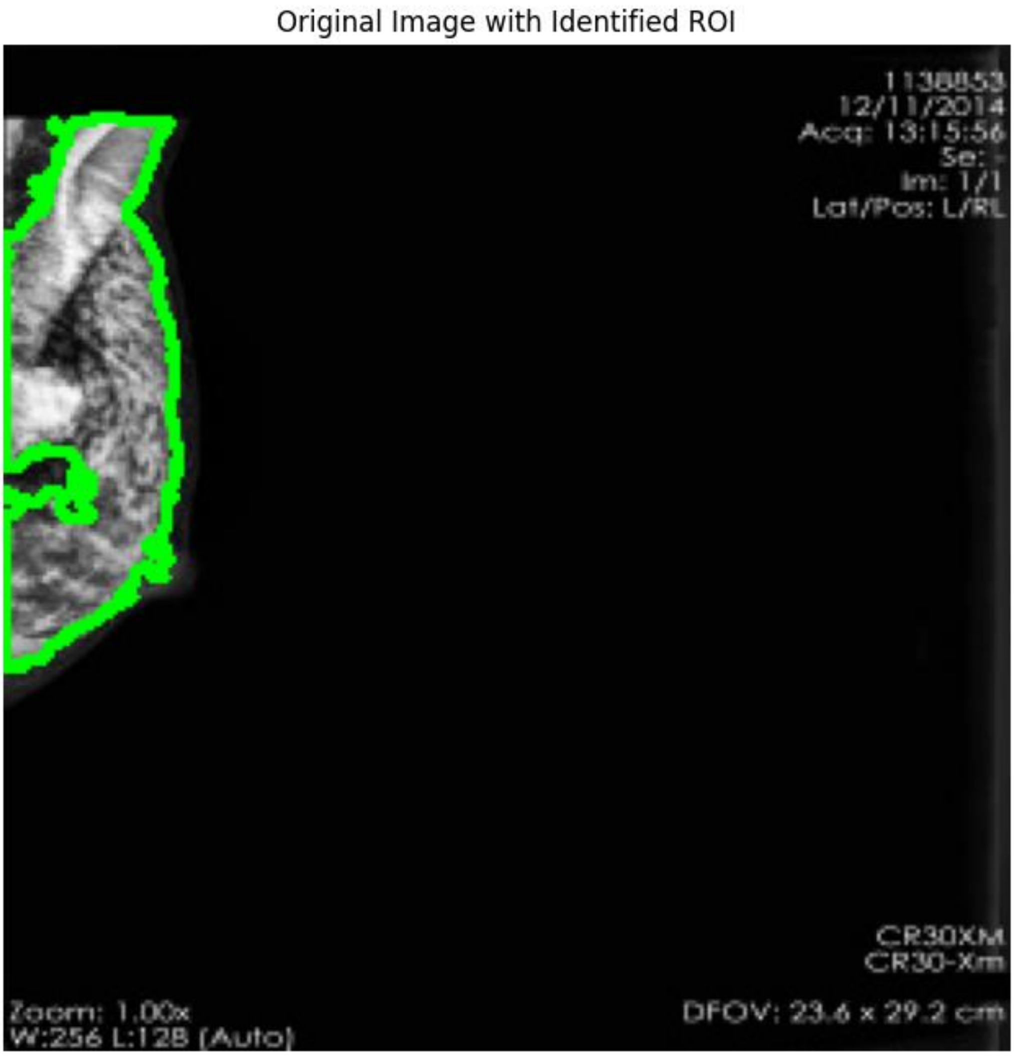

Fig. 11 ROI Identification and Property Extraction

For ROI extraction, an initial segmentation of candidate tumor regions was conducted by applying Otsu's thresholding, which automatically selects an optimal global threshold value (68.0) separating foreground and background pixels. The binarized image, shown in Fig. 11, was subsequently analyzed with connected component analysis whereby the distinct objects were identified and labeled, from which the largest non-background component was selected as the main Region of Interest (ROI) corresponding to the prominent tumor-like structure. Based on this ROI, region properties have been calculated from which geometric and shape features were extracted: area (total number of pixels in the region), perimeter (length of the object boundary), eccentricity (degree of elongation), major axis length (longest diameter of equivalent ellipse), minor axis length (shortest diameter of an equivalent ellipse), and compactness, a measure of shape regularity, is defined by Eq. (1).

$$\text{Compactness} = 4\pi \times \text{Area} / \text{Perimeter}^2 \quad (1)$$

These characteristics are important quantitative information on the tumor size, geometry and regularity, which contribute to an effective tumor subclassification. Specifically, in the example ROI, the computed properties are an area of 4353.0 pixels, a perimeter of 514.96 pixels, and a compactness value of 0.2063.

5.8 Explained Variance Ratio by Principal Components

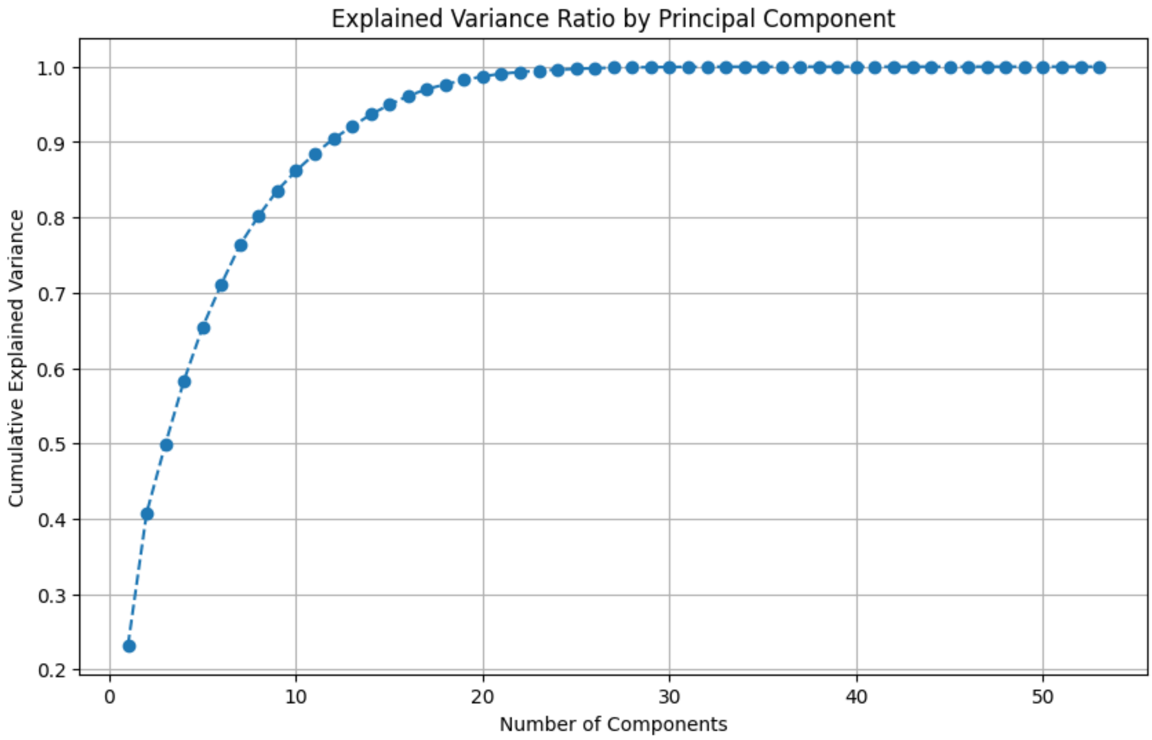

Fig. 12 Explained Variance Ratio by Principal Components

The Explained Variance Ratio by Principal Components plot is a key diagnostic in PCA used to ascertain quantitatively how many principal components are needed in order to retain a high percentage of information from the original dataset and yet reduce dimensionality, shown in Fig. 12. Each of these principal components is calculated as a linear combination of the features, and they account for a decreasing amount of variance, which is displayed in one explained variance ratio. The total amount of variance accounted for is shown by a monotonically increasing curve known as cumulative explained variance; each point plotted on the curve represents the sum of variances with an increased number of principal components. In a feature matrix **X** where rows correspond to samples and columns represent features, PCA involves finding the eigenvalues λ_j and eigenvectors (principal components) of its covariance matrix. The relative portion of the explained variance by the j^{th} component is defined by Eq. (2).

$$\text{Explained Variance Ratio} = \lambda_j / (\Sigma_k \lambda_k) \quad (2)$$

where $\Sigma_k \lambda_k$ represents the sum of all eigenvalues.

In our multimodal model framework, this interpretation was important to the purpose of reducing features from an initial

53 (all combined preprocessed clinical and holistic DSP derived images). The added plot directly showed 16 could be chosen as the principal components and would cover about 95% of total variation. This judicious dropping of dimensionality from 53 to 16 is important. It is an efficient way to statutorily alleviate the dimensionality curse and reduce computational loads of deep learning model, also it can wash out noise or collinearity in data, and therefore improve generalization capability and interpretability of a model albeit with little waste.

6 Deep Learning Model

6.1 Deep Learning Model Architecture

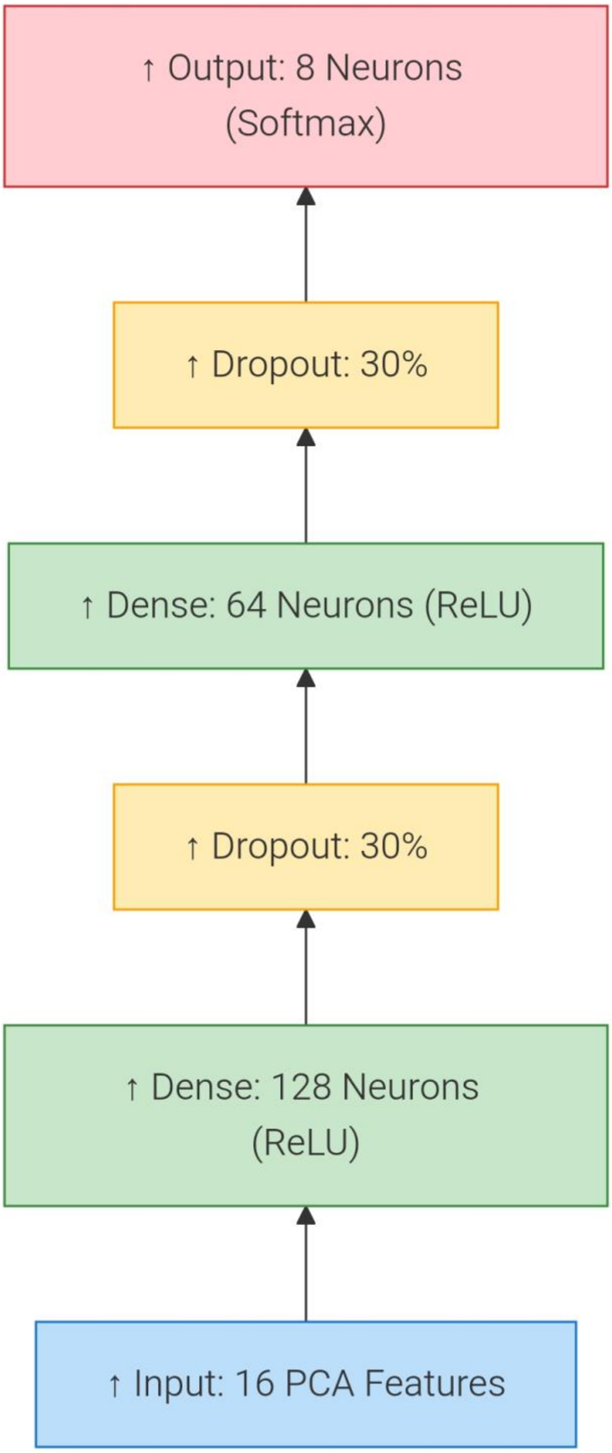

Fig. 13 Architecture of the Deep Learning Model

The proposed multi-modal deep learning framework, shown in Fig. 13, uses a Multi-Layer Perceptron (MLP) network to subclassify the benign breast tumors. The sequential model is intended for the input data of a reduced dimensionality feature set consisting of 16 Principal Component Analysis (PCA) resulting from composite features based on clinical and DSP-extracted image features.

The architecture is organized as follows: The model takes 16 input features from the input layer that is set up to take a vector of 16 numerical features, with this vector representing the principal components that enclose around 95% of the variance from the complete multimodal dataset. This is succeeded by a first hidden layer, which is a dense (fully connected) layer with 128 neurons performing linear transformation on input and applying a Rectified Linear Unit (ReLU) activation function for non-linearity. In order to avoid overfitting, a first dropout layer with a rate of 0.3 dropping ratio is enforced right after the first hidden layer, randomly deactivating 30% of input units during training. The network then enters into a second hidden layer, which is a dense layer with 64 neurons that also employs the ReLU activation function as output for additional computation. A second dropout layer with a rate of 0.3 is added for more regularization. Last but not least, the output layer contains neurons corresponding to the benign breast tumor subclasses. This layer uses the softmax activation function to convert raw output scores into class probabilities.

6.2 Model Compilation

The model is optimized using the Adam optimizer, which was selected because of its adaptive learning rate. The well-known loss function, categorical cross-entropy, is used, which is appropriate for multi-class classification problems with one-hot encoded targets. The main metric used to monitor the process of training and evaluation is accuracy, i.e., performance (the fraction of correct classifications).

7 RESULTS

7.1 Training and Validation Performance

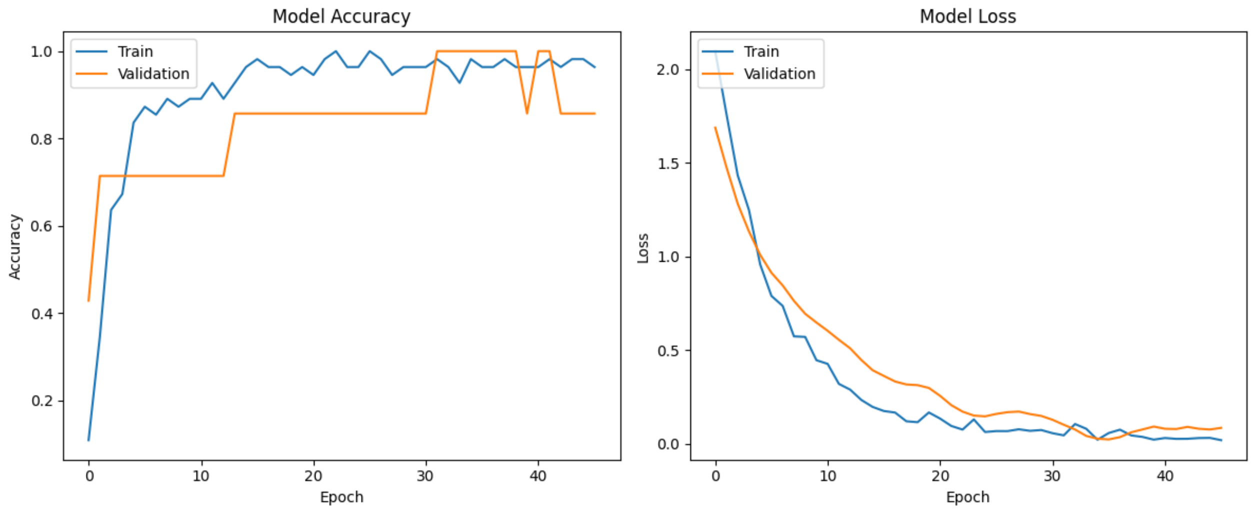

Fig. 14 Training and Validation Accuracy and Loss Curves

The performance of the model is evaluated on these popular metrics; specifically, in deep learning there are multiple evaluation parameters, such as accuracy and reading trends from the validation curve. Fig. 14 shows the training and validation accuracy and loss curves. For our incoming model, accuracy gives us directly the counting of correct predictions over all predictions, which provides its prediction ability. In our case a test accuracy of 1.0000 means that the model perfectly classified all observations within the independent test sample of data. This measure makes it easy to understand the accuracy, but the interpretation can be challenged by observing how well a model learns by visualizing validation curves. These curves represent a selected metric (often loss or accuracy) as a function of how long the network has been training, in this case number of epochs. In the context of the MLP model, for example, the validation curve shows how the model has been gradually optimized and eventually settles with validation accuracy that achieves a slight improvement up to 1.0000 at Epoch 32, while test loss stopped down at 0.0116. This is a good sign; here we would like to see both training and validation curves reaching maximum/optimal value simultaneously with minimal change. If the improvement extended to training performance but not to validation, however, then that is an indicator of overfitting—it indicates that the model learned some noise in the training data and was harmed thereby. Conversely, if the model were performing poorly on both curves consistently, it might be underfitting. This trajectory, with both metrics converging to nearly perfect values, suggests a good generalization of the model from training data to unseen validation and test examples and a solid learning process within the problem's context.

7.2 Model Performance

The trained MLP model delivered outstanding performance on the test set, reaching a test loss of 0.0116 and a test accuracy of 1.0000.

8 Conclusion

This research successfully implemented and tested an innovative multi-modal deep learning architecture for subclassification of benign breast tumors. By carefully combining medical (clinical, histopathological) and mammogram data in a series of advanced DSP (digital signal processing) steps, an efficient means to derive meaningful features and achieve high diagnostic accuracy was presented.

The framework started by performing large-scale preprocessing (noise reduction: median and Gaussian filtering; contrast enhancement: CLAHE and histogram equalization; intensity normalization; quadratic resizing) to prepare the mammograms for deep processing. Thereafter, a highly comprehensive set of DSP-based features were applied to the images to explore their frequencies (FFT), time-frequencies (DWT), texture (GLCM, LBP), spatial domain filtered contents (Canny, LoG), and morphological/ROI features. Clinical and pathological information was carefully pre-processed by addressing missing values as well as performing one-hot encoding. All these varied features were aggregated before principal component analysis (PCA) was conducted to manage dimensionality, resulting in a 16-dimensional feature space when considering the top 95% of variability by PCA.

For overcoming the issues of small medical datasets, DSP-domain data augmentation approaches (frequency noise and wavelet perturbation) were successfully applied, resulting in a significantly increased data size with 160 augmented images produced. A deep learning model constructed in an MLP architecture (input, hidden layers with ReLU activation and dropout for regularization, and output) was trained on this combined and downsampled set.

Of critical importance, the performance of our model on the test set was remarkable, with a test loss at 0.0116 and an impressive test accuracy of 1.0000. This result highlights the combined advantages of multimodal with advanced DSP and deep learning for challenging medical classification tasks. Using a numerical, objective, and quantitative framework for benign breast tumor subclassification might help physicians in accurate diagnosis and patient management.

These findings are very encouraging; however, it should be noted that the dataset is very small. Another limitation for generalization is attributable to non-stratified sampling splitting with scarce classes. Hence, in the future we will validate such a framework using larger, more diverse, and independent datasets to ensure that it is robust and generalizable. Moreover, including these generated DSP-domain augmented images directly in the training pipeline is likely to improve the model's robustness on unseen data as well. The discoveries from our study indirectly provide evidence for a more refined AI-powered diagnostic system in benign breast tumor histopathology.

References

[1] Manish Joshi, Aparna Bhale, Unmesh Takalkar, "Benign Breast Tumor Dataset", IEEE Dataport, May 9, 2021, doi:https://doi.org/10.21227/6sda-hn78 [Accessed on: 03 January 2026]

Shahinur Rahman (full name: Shahinur Islam Kowser) has completed his Bachelor of Science (B.Sc.) in Electrical and Electronic Engineering (EEE) from City University, Bangladesh. His primary academic and research focus is on power systems, with particular emphasis on power system analysis, protection, and modern smart grid technologies. He works on Deep Learning and Digital Signal Processing (DSP) applications in power systems, especially for smart grid monitoring, protection, and intelligent energy analytics.